

Structural Polymorphism in Amyloids

NEW INSIGHTS FROM STUDIES WITH Y145Stop PRION PROTEIN FIBRILS^{*[5]}

Received for publication, September 8, 2011, and in revised form, October 5, 2011. Published, JBC Papers in Press, October 15, 2011, DOI 10.1074/jbc.M111.302539

Eric M. Jones^{†1}, Bo Wu[§], Krystyna Surewicz[‡], Philippe S. Nadaud[§], Jonathan J. Helmus[§], Shugui Chen[‡], Christopher P. Jaronic^{§2}, and Witold K. Surewicz^{‡3}

From the [†]Department of Physiology and Biophysics, Case Western Reserve University, Cleveland, Ohio 44106 and [§]Department of Chemistry, The Ohio State University, Columbus, Ohio 43210

Background: The Y145Stop prion protein is a useful model for understanding basic principles of amyloid formation.

Results: Deletion of the conserved palindrome sequence ¹¹³AGAAAAGA¹²⁰ results in an altered amyloid β -core without affecting amyloidogenicity or seeding specificity.

Conclusion: The core of some amyloids contains “essential” (nucleation-determining) and “nonessential” regions.

Significance: This study reveals a novel mechanism for structural polymorphism in amyloids.

The C-terminally-truncated human prion protein variant Y145Stop (or PrP23–144), associated with a familial prion disease, provides a valuable model for studying the fundamental properties of protein amyloids. In previous solid-state NMR experiments, we established that the β -sheet core of the PrP23–144 amyloid is composed of two β -strand regions encompassing residues \sim 113–125 and \sim 130–140. The former segment contains a highly conserved hydrophobic palindrome sequence, ¹¹³AGAAAAGA¹²⁰, which has been considered essential to PrP conformational conversion. Here, we examine the role of this segment in fibrillization of PrP23–144 using a deletion variant, Δ 113–120 PrP23–144, in which the palindrome sequence is missing. Surprisingly, we find that deletion of the palindrome sequence affects neither the amyloidogenicity nor the polymerization kinetics of PrP23–144, although it does alter amyloid conformation and morphology. Using two-dimensional and three-dimensional solid-state NMR methods, we find that Δ 113–120 PrP23–144 fibrils contain an altered β -core extended N-terminally to residue \sim 106, encompassing residues not present in the core of wild-type PrP23–144 fibrils. The C-terminal β -strand of the core, however, is similar in both fibril types. Collectively, these data indicate that amyloid cores of PrP23–144 variants contain “essential” (*i.e.* nucleation-determining) and “nonessential” regions, with the latter being “movable” in amino acid sequence space. These findings reveal an intriguing new mechanism for structural polymorphism in amyloids and suggest a potential means for modulating the physicochemical properties of amyloid fibrils without compromising their polymerization characteristics.

The amyloid family of protein structures continues to intrigue researchers in both the chemical and biomedical disciplines. Amyloids, which are defined classically (1) as large, β -sheet rich protein assemblies having a characteristic “cross- β ” x-ray diffraction pattern, a tendency to bind dyes such as thioflavin T, and usually a fibrous morphology, have attracted much attention in recent decades for their role in human diseases such as systemic amyloidoses (2), type 2 diabetes (3), and neurodegenerative disorders such as Alzheimer, Huntington, and the prion diseases (1, 4, 5). However, amyloids are also of fundamental interest, as amyloid proteins have been found integral to such diverse biological processes as biofilm formation and fungal spore dispersal (1, 6–8). Moreover, the realization that non-native amyloids can be formed by hundreds of widely divergent proteins and peptides has led to reconsideration of the fundamental principles of protein stability and folding (9, 10).

Both the functional and deleterious aspects of amyloid stem from the variability in the structure and stability of the fibril state (1, 7, 10, 11) and from the diversity of smaller, often toxic assembly intermediates (5, 12). For the past several years, our laboratory has used the recombinant truncated prion protein (PrP)⁴ variant PrP23–144 (also known as Y145Stop PrP), associated with a familial prion disease (13), as a model system for understanding the structural principles underlying amyloid seeding capability and structural polymorphism (14–17). Structural studies by solid-state NMR spectroscopy (18–20) have shown that PrP23–144 amyloid contains two β -strands spanning residues \sim 113–125 (with a break at positions \sim 116–117) and a third strand involving residues \sim 130–140 (numbering according to human PrP). The latter strand contains a species-specific sequence at residues 138–139 that determines seeding specificity (15, 16). The former β -strand region, conversely, encompasses a conserved hydrophobic palindrome sequence, ¹¹³AGAAAAGA¹²⁰, which has been shown critical for amyloidogenesis of certain PrP peptides (21–23) and for propagation of pathological PrP in cell culture (24). However,

* This work was supported by National Institutes of Health Grants R01NS038604 and R01NS044158 (to W. K. S.) and R01GM094357 (to C. P. J.).

[5] The on-line version of this article (available at <http://www.jbc.org>) contains supplemental “Experimental Procedures,” Table S1, Figs. S1–S6, and additional references.

¹ Present address: Department of Chemistry, University of Washington, Seattle, WA 98195.

² To whom correspondence may be addressed: Dept. of Chemistry, The Ohio State University, Columbus, OH 43210. Tel.: 614-247-4284; Fax: 614-292-1685; E-mail: jaronic@chemistry.ohio-state.edu.

³ To whom correspondence may be addressed: Dept. of Physiology and Biophysics, Case Western Reserve University, Cleveland, OH 44106. Tel.: 216-368-0139; Fax: 216-368-1307; E-mail: witold.surewicz@case.edu.

⁴ The abbreviations used are: PrP, prion protein; PrP23–144, prion protein fragment containing residues 23–144.

Polymorphism in Y145Stop Prion Protein Amyloids

given that C-terminal truncated Y145Stop PrP fragments containing the palindrome do not form amyloid in the absence of residues 138–139 (14), we questioned whether residues 113–120 are in fact critical for amyloid formation by PrP23–144, despite being incorporated into the fibril core. We have therefore studied amyloid formation and propagation by the Δ 113–120 PrP23–144 variant lacking the hydrophobic 113–120 palindrome and characterized the resulting fibrils by microscopic and spectroscopic methods. Surprisingly, deletion of residues 113–120 (which removes a significant portion of the β -sheet-forming region of wild-type PrP23–144) does not abolish amyloid formation or seeding capability, although it does alter the fibril conformation. Even more interesting, solid-state NMR reveals that several residues that are unstructured in WT PrP23–144 fibrils become incorporated into the core of the Δ 113–120 PrP23–144 amyloid, whereas the C-terminal β -strand is largely conserved in both proteins. These results reveal a new mechanism for structural polymorphism in amyloid fibrils and indicate that certain amyloids may contain both “essential” (nucleation-determining) and “nonessential” parts in the β -core. Modification of the latter via evolution or biotechnology may provide a means of altering amyloid physical properties without compromising nucleation activity.

EXPERIMENTAL PROCEDURES

Protein Expression and Purification—The vector encoding human PrP23–144 (Met-129 polymorph) has been described previously (14). Plasmid cDNA encoding Δ 113–120 PrP23–144 was produced by deletion mutagenesis on the wild-type template using a QuikChange kit (Stratagene). Natural abundance and ^{13}C , ^{15}N -labeled WT and Δ 113–120 PrP23–144 were expressed in *Escherichia coli* and purified by nickel ion affinity chromatography as described previously (18, 25). After cleavage of the histidine tag, proteins were dialyzed exhaustively against Milli-Q water, lyophilized, and stored at 4 °C until use. Purity of all proteins was better than 95% as judged by SDS-PAGE, and their identity was confirmed by MALDI mass spectrometry.

Kinetics of Fibrillization of PrP23–144—PrP23–144 variants were fibrillized as described (14). Briefly, lyophilized protein was dissolved in Milli-Q water, and fibril formation was induced by addition of 1 M potassium phosphate (pH 6.4) to a final concentration of 50 mM. The final protein concentration was 400 μM , and all samples contained protease inhibitors (Sigma). Periodically, 5- μl portions of protein solution were withdrawn from each specimen and added to 500 μl of 10 μM thioflavin T, pH 6.4, in a 5-mm path length cuvette, and thioflavin T fluorescence (excitation, 450 nm; emission, 482 nm) was measured using an SLM 8100 spectrofluorometer. For seeded experiments, 5% (w/w) pre-formed amyloid fibrils were added to the reaction mixture immediately after reconstituting protein in buffer. All experiments were repeated a minimum of five times.

Atomic Force Microscopy—Atomic force microscopy images were obtained exactly as described previously (14). Images were acquired in both height and amplitude modes and were processed by plane fitting and low pass filtering.

FTIR Spectroscopy—Infrared spectra of PrP23–144 variants were obtained as described (14, 16, 26), using protein samples prepared in deuterium oxide instead of water. To resolve overlapping component bands in the amide I' region, all spectra were Fourier self-deconvoluted, using parameters equivalent to a 15 cm^{-1} peak half-width and resolution enhancement factor of 1.6.

Solid-state NMR Spectroscopy—NMR data were collected on a 500 MHz Varian spectrometer equipped with a 3.2 mm Varian BioMAS probe. The magic-angle spinning frequency was controlled at 11.111 kHz \pm \sim 3 Hz, and the effective sample temperature was actively regulated at \sim 5 °C. A suite of two-dimensional and three-dimensional NMR experiments, including two-dimensional ^{15}N - $^{13}\text{C}^{\alpha}$, ^{13}C - ^{13}C , ^{15}N -($^{13}\text{C}^{\alpha}$)- $^{13}\text{C}\text{X}$, and ^{15}N -($^{13}\text{C}'$)- $^{13}\text{C}\text{X}$ and three-dimensional ^{15}N - $^{13}\text{C}^{\alpha}$ - $^{13}\text{C}\text{X}$, ^{15}N - $^{13}\text{C}'$ - $^{13}\text{C}\text{X}$, and $^{13}\text{C}'$ - ^{15}N - $^{13}\text{C}^{\alpha}$ was used to establish the resonance assignments of Δ 113–120 human PrP23–144 amyloid fibrils; typical parameters and experimental details can be found elsewhere (18, 27). All NMR data were processed in NMRPipe (28) and analyzed using Sparky (29).

RESULTS

Deletion of Residues 113–120 Does Not Affect PrP23–144 Amyloidogenesis—We questioned whether deletion of the palindrome sequence $^{113}\text{AGAAAAGA}^{120}$ of human PrP, which composes a part of the β -sheet core of PrP23–144 amyloid (18–20) and forms amyloid in isolation (21), would abolish amyloid formation by PrP23–144. To this end, formation of WT PrP23–144 amyloid (designated [WT]) and Δ 113–120 PrP23–144 amyloid (designated [Δ 113–120]) was monitored using the fluorometric thioflavin T assay as described previously (14). Surprisingly, the kinetics of fibril formation by both proteins were very similar, with lag phases of 3.6 ± 0.5 h and 3.5 ± 0.9 h for [WT] and [Δ 113–120] amyloids, respectively (Fig. 1A). Furthermore, in each case, addition of 5% (w/w) pre-formed fibrils to the solution of monomeric protein completely eliminated the lag phase, consistent with a nucleation-dependent mechanism of amyloidogenesis. We thus conclude that residues 113–120, despite being a part of the β -sheet core in PrP23–144 amyloid, are not essential for fibril formation.

Previous work on PrP23–144 variants established that amyloid formed from one protein sequence is often able to seed conversion of protein of another sequence, provided that the soluble protein is capable of adopting the conformation present in a critical (*i.e.* nucleation-determining) region of the amyloid seed (16). To test the role of residues 113–120 as potential determinant of seeding specificity, we performed cross-seeding experiments using the thioflavin T assay. As shown in Fig. 1, B and C, we found that addition of pre-formed fibrillar seed of either [WT] or [Δ 113–120] amyloid to soluble protein of the other sequence results in effective seeding of conversion with total elimination of the lag phase of amyloidogenesis. Thus, residues 113–120 appear to be outside the critical nucleation-determining region of PrP23–144 amyloid.

Wild-type and Δ 113–120 PrP23–144 Fibrils Display Different Structural Characteristics—Given the intriguing finding that the deletion of residues that form part of the β -sheet core in PrP23–144 fibrils does not abolish fibril formation, we

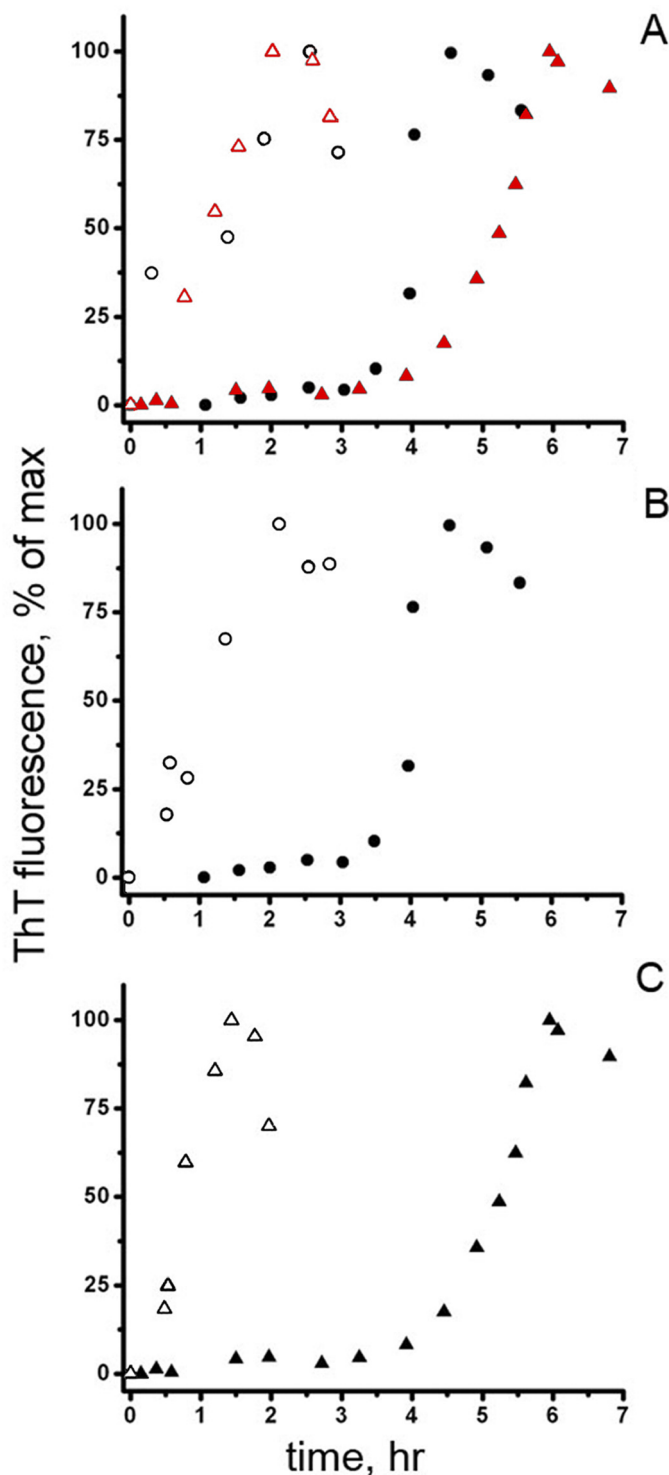


FIGURE 1. Deletion of residues 113–120 from PrP23–144 does not affect amyloidogenesis or cross-seeding capability. *A*, kinetics of amyloid formation (thioflavin T (*ThT*) fluorescence) of WT (black circles) or Δ 113–120 (red triangles) PrP23–144, in the absence (filled symbols) or presence (open symbols) of 5% (w/w) pre-formed amyloid seed of the same sequence. *B*, kinetics of WT PrP23–144 amyloidogenesis in the absence (filled symbols) or presence (open symbols) of 5% (w/w) Δ 113–120 amyloid. *C*, kinetics of Δ 113–120 PrP23–144 amyloidogenesis in the absence (filled symbols) or presence (open symbols) of 5% (w/w) [WT] amyloid. As noted previously (15), after reaching its maximum, thioflavin T fluorescence often shows a time-dependent decrease, likely due to clumping of individual PrP23–144 fibrils.

addressed the issue of the structural consequences of this deletion. To this end, the ultrastructure of [WT] and Δ 113–120 fibrils was examined by atomic force microscopy and the secondary structure of these fibrils was assessed using Fourier transform infrared spectroscopy. Although low resolution images of fibrils formed by both proteins appear similar (Fig. 2, *A* and *B*), higher resolution amplitude mode images of individual fibrils (Fig. 2, *C* and *D*) show that deletion of residues 113–120 has a considerable effect on PrP23–144 fibril morphology. As noted previously (14, 16), [WT] fibrils (Fig. 2*D*) exhibit a “bead-like” segmented morphology with a \sim 30 nm axial period. By contrast, Δ 113–120 fibrils were found to have a left-handed helical morphology with some variation in the period of the helical twist, even along a single fibril. The period was most frequently \sim 70 nm, but ranged from 45 nm to 100 nm. (A representative fibril is shown in Fig. 2*C*.) Moreover, although [WT] fibrils have a relatively uniform thickness of \sim 5 nm as shown in earlier work (16), Δ 113–120 fibrils are generally thinner (*i.e.* of smaller vertical dimension in height-mode images) and tended toward a bimodal distribution of fibril thicknesses, suggestive of a hierarchical mechanism of assembly. Fig. 2*E* shows a height mode image of a few Δ 113–120 fibrils; height sections through two of these fibrils (along lines *ab* and *cd*) are plotted in Fig. 2*F*. The thin fibril (line *cd* in Fig. 2*E*, gray in Fig. 2*F*) has a mean thickness of \sim 2 nm (this is the type of fibril shown in Fig. 2*C*); fibrils thinner than this were never observed. The thick fibril (line *ab*, black) has a mean thickness of \sim 4–5 nm, roughly twice that of the thin fibril, with a similar helical period. This observation raises the possibility that thicker Δ 113–120 fibrils form via association of thin Δ 113–120 fibrils (protofilaments), and this was, in fact, observed in a few atomic force microscopy fields (Fig. 2*G*). Such hierarchical assembly was never observed for [WT] amyloid (14, 16). Thus, deletion of residues 113–120 greatly affects not only the morphology but also the assembly mechanism of PrP23–144 amyloid fibrils.

These ultrastructural data are mirrored in FTIR spectra (Fig. 3), which report on protein secondary structure. Whereas both WT and Δ 113–120 PrP23–144 exhibit a single broad amide I' band centered at \sim 1648 cm^{-1} in soluble form, consistent with disordered secondary structure (30), these proteins show distinct spectra in the fibrillar state. [WT] fibrils contain peaks corresponding to β -sheet at 1628 and 1639 cm^{-1} as shown previously (14, 16, 26), whereas Δ 113–120 fibrils have only a single β -sheet band at 1625 cm^{-1} . Both fibril types also contain some disordered structure (evident as a peak at 1648–1649 cm^{-1}), consistent with previous solid-state NMR results (18, 19). Thus, deletion of residues 113–120 appears to have a considerable effect on the type of β -sheet structure present in PrP23–144 amyloids.

Solid-state NMR Reveals Alternate β -Sheet Core for Δ 113–120 PrP23–144 Fibrils—Previously, we used solid-state NMR spectroscopy to characterize the β -core region in PrP23–144 amyloid at the molecular level (18–20). To gain higher resolution insight into the structural consequences of deletion of the $^{113}\text{AGAAAAGA}^{120}$ palindrome sequence, we performed a series of two-dimensional and three-dimensional solid-state NMR experiments to identify the location of secondary struc-

Polymorphism in Y145Stop Prion Protein Amyloids

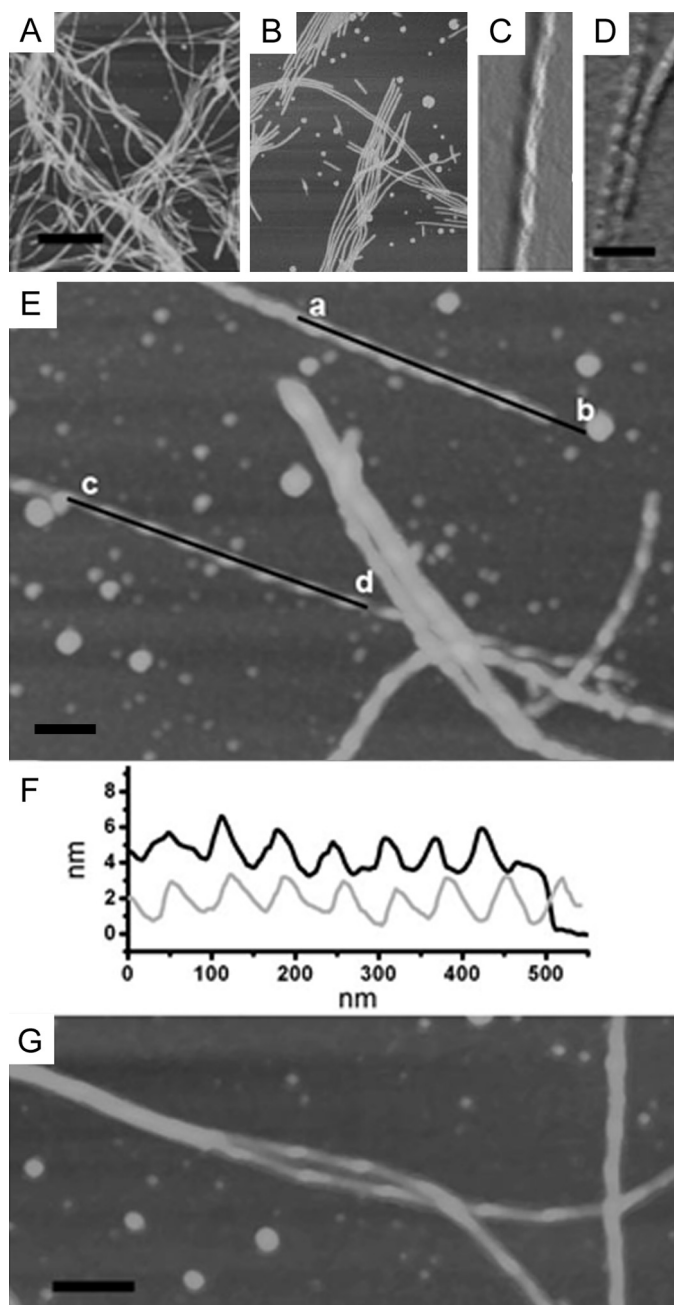


FIGURE 2. Atomic force microscopy images of [WT] and [Δ113–120] amyloid fibrils. A and B, low resolution height-mode images of [Δ113–120] (A) and [WT] (B) fibrils (scale bar, 500 nm; applies to both panels). C and D, high resolution amplitude-mode images of [Δ113–120] (C) and [WT] (D) fibrils (scale bar, 100 nm; applies to both panels). E, high resolution height mode image of [Δ113–120] fibrils, showing both thin and thick helical fibrils. F, section through the thick (black line) or thin (gray line) fibrils corresponding to lines *ab* or *cd*, respectively, in E (scale bar, 100 nm). G, height mode image of two thin [Δ113–120] fibrils winding together to form a thick fibril (scale bar, 100 nm).

ture elements within [Δ113–120] amyloid fibrils. The two-dimensional ^{15}N - $^{13}\text{C}^\alpha$ chemical shift correlation spectra of uniformly ^{13}C , ^{15}N -labeled [WT] (red contours) and [Δ113–120] fibrils (blue contours) recorded under identical experimental conditions are shown in Fig. 4A. The spectrum for [Δ113–120] fibrils contains only a small subset of the expected ^{15}N - $^{13}\text{C}^\alpha$ correlations (28 of 118), with ^{15}N and ^{13}C line widths compa-

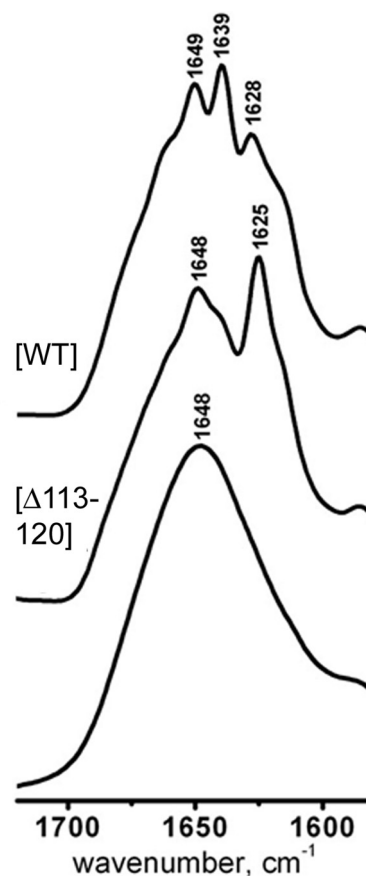


FIGURE 3. FTIR spectra (amide I' band) showing differences in secondary structure between soluble WT PrP23–144 (bottom), [Δ113–120] fibrils (middle), and [WT] fibrils (top). The FTIR spectrum of soluble Δ113–120 is indistinguishable from that of WT protein. All spectra were band-narrowed by Fourier self-deconvolution as described in the text.

able to [WT] material. Thus, akin to [WT] fibrils, [Δ113–120] amyloid consists of a compact, highly ordered, and relatively rigid core region and a large domain subject to considerable dynamics (18, 19). However, there appear to be major conformational differences in the core regions of these two amyloids. This is indicated by (i) the very small degree of overlap between the ^{15}N - $^{13}\text{C}^\alpha$ spectra for the two proteins and (ii) the same number of cross-peaks detectable in spectra for [WT] and [Δ113–120] fibrils, despite the deletion of eight amyloid core residues from the PrP23–144 sequence. The latter finding strongly suggests that additional amino acids (*i.e.* not contributing to the core of [WT] fibrils) become sufficiently immobilized and incorporated into the core region of [Δ113–120] fibrils.

Sequential resonance assignments for the Δ113–120 PrP23–144 amyloid core residues (established primarily on the basis of three-dimensional ^{15}N - $^{13}\text{C}^\alpha$ - $^{13}\text{C}^\beta$, ^{15}N - $^{13}\text{C}'$ - $^{13}\text{C}^\beta$, and $^{13}\text{C}'$ - ^{15}N - $^{13}\text{C}^\alpha$ correlation spectra) are summarized in supplemental Table S1, and strips from three-dimensional solid-state NMR data sets displaying the protein backbone connectivity are shown in supplemental Fig. S1. Similarly to the [WT] amyloid, the rigid core region for [Δ113–120] fibrils is located near the C terminus, between amino acids ~106–141. Interestingly, however, upon deletion of the $^{113}\text{AGAAAAGA}^{120}$ sequence, several residues (amino acids ~106–111) located just outside the amy-

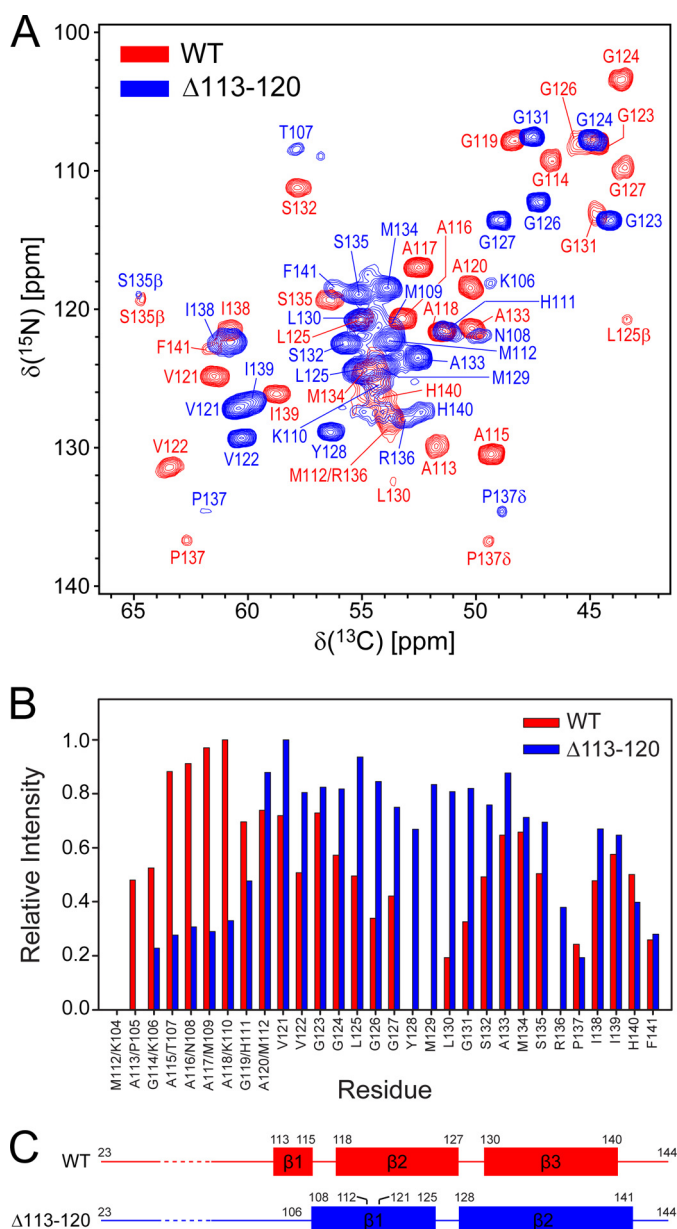


FIGURE 4. Solid-state NMR analysis of WT and $\Delta 113-120$ PrP23-144 amyloid fibrils. *A*, two-dimensional $^{15}\text{N}-^{13}\text{C}^{\alpha}$ spectra of [WT] fibrils (red contours) and $[\Delta 113-120]$ fibrils (blue contours) recorded at 11.7 Tesla, 11.111 kHz magic-angle spinning rate and an effective sample temperature of $\sim 5^{\circ}\text{C}$. Each spectrum was collected with acquisition times of 15 and 28 ms in t_1 and t_2 , respectively, and a measurement time of ~ 8 h. *B*, cross-peak intensities in two-dimensional $^{15}\text{N}-^{13}\text{C}^{\alpha}$ spectra of [WT] fibrils (red) and $[\Delta 113-120]$ fibrils (blue) shown in *A* as a function of residue number. Peak intensities were obtained using Sparky and are normalized according to the most intense correlation in each spectrum. *C*, secondary structure of the amyloid core region in [WT] fibrils (red) and $[\Delta 113-120]$ fibrils (blue) predicted using TALOS+ (31). To facilitate the comparison of amyloid core regions for [WT] and $[\Delta 113-120]$ fibrils, the protein C termini were aligned.

loid core region for WT PrP23-144 are included in the $[\Delta 113-120]$ fibril core. Moreover, residues Tyr-128–Leu-130, which are located in the middle of WT PrP23-144 core region but are either undetectable or display weak cross-peak intensities in [WT] spectra due to increased flexibility, give rise to intense correlations for $[\Delta 113-120]$ fibrils. A quantitative comparison of relative cross-peak intensities in $^{15}\text{N}-^{13}\text{C}^{\alpha}$ spectra of [WT] and $[\Delta 113-120]$ amyloid (Fig. 4*B*) reveals that, in stark contrast

to WT protein, most residues in the central part of the core (amino acids $\sim 111-140$) exhibit strong and relatively uniform correlations for $[\Delta 113-120]$ fibrils. (Several amino acids found at or near the edges of the $[\Delta 113-120]$ amyloid core, including amino acids $\sim 106-110$ and 141, show attenuated cross-peak intensities due to elevated conformational dynamics as observed previously for [WT] fibrils (18, 19).)

Altogether, these findings indicate that the slow, microsecond-millisecond time scale protein backbone motions that appear to be present throughout the core region for WT PrP23-144 fibrils (19) are effectively quenched in $[\Delta 113-120]$ amyloid, suggesting that deletion of the palindrome sequence results in a considerable rearrangement of the PrP23-144 amyloid core structure. Indeed, this notion is consistent with the substantial (up to ~ 5 ppm) differences observed for many $^{13}\text{C}'$, $^{13}\text{C}^{\alpha}$ and $^{13}\text{C}^{\beta}$ chemical shifts (which are sensitive reporters of local protein structure; supplemental Fig. S2) for residues Val-121–Phe-141, which are part of the amyloid core in both [WT] and $[\Delta 113-120]$ fibrils. We note here that the assignment of residues 106–108 was complicated by attenuated resonance intensities and is somewhat tentative (see supplemental text and Fig. S3).

The ^{13}C and ^{15}N chemical shifts were employed to predict the protein backbone conformation in the core regions of [WT] and $[\Delta 113-120]$ fibrils using the TALOS+ program (31) in the “no proton” mode. A summary of the secondary structure analysis is shown in Fig. 4*C*, and supplemental Figs. S4 and S5 show plots of the $^{13}\text{C}'$, $^{13}\text{C}^{\alpha}$, and $^{13}\text{C}^{\beta}$ secondary chemical shifts and predicted backbone φ and ψ torsion angles and normalized probabilities of the different secondary structure elements, respectively. For [WT] fibrils, this analysis indicates the presence of three β -strands, a short strand between residues $\sim 113-115$ and two longer strands encompassing residues $\sim 118-127$ and $\sim 130-140$, interrupted by two regions of non- β -structure, with one of these regions containing the flexible Tyr-128 and Met-129 residues. These results generally are consistent with our previous analysis of the secondary structure in the core region of [WT] fibrils (18) using other chemical shift-based approaches, although the present data reveal that the second strand is likely extended by several residues. By contrast, upon deletion of the $^{113}\text{AGAAAAGA}^{120}$ sequence, the secondary structure analysis indicates that the amyloid core region in $[\Delta 113-120]$ fibrils extends N-terminally up to residue ~ 106 , consisting of only two β -strands of nearly equal length, encompassing residues $\sim 108-125$ (with residues 113–120 missing) and $\sim 128-141$. Although the latter strand is nearly coincident with the C-terminal strand in [WT] fibrils, the first strand of $[\Delta 113-120]$ fibrils encompasses multiple residues that are flexible and of undefined structure in the [WT] amyloid but conserves the approximate size of the N-terminal β -region seen in [WT] fibrils. Thus, a portion of the β -sheet core in PrP23-144 amyloid is “movable” in amino acid sequence space; that is, residues ordinarily excluded from the amyloid core may become incorporated into the core if sequences with a stronger propensity to form intermolecular β -sheet are absent.

The properties of [WT] and $[\Delta 113-120]$ fibrils were also analyzed by limited proteolysis with proteinase K. Consistent with previous data (32), proteinase K treatment of [WT] fibrils

Polymorphism in Y145Stop Prion Protein Amyloids

resulted in a ~4.5-kDa fragment as judged by SDS-PAGE. A similar, though slightly smaller fragment was observed for [Δ 113–120] fibrils (supplemental Fig. S6A). Mass spectrometric analysis revealed three major proteinase K-resistant fragments with molecular masses of 4671, 4799, and 4886 Da and 4131, 4259, and 4346 Da for [WT] and (113–120) fibrils, respectively (supplemental Fig. S6B). In each case, these masses could be matched to residues 97/98/99–144. These data are generally consistent with the identity of the ordered, β -sheet core as determined precisely by solid-state NMR. Somewhat longer proteinase K-resistant regions compared with β -sheet cores (and the same cleavage sites for [WT] and (113–120) fibrils may be explained by factors such as residual order in the region(s) adjacent to β -core and steric constraints limiting the access of large proteinase K molecules (~29 kDa) to potential cleavage sites near the edges of the core.

DISCUSSION

Essential and Nonessential Regions of PrP23–144 Amyloid Core—Many studies of prion amyloidogenicity and infectivity have identified the strictly conserved hydrophobic palindrome ¹¹³AGAAAAGA¹²⁰ (numbering according to human PrP) as a putative fibrillogenic sequence, essential for cellular propagation of infectious PrP (24). Indeed, this sequence has been found to form amyloid in isolation (21), and structural models for amyloids of several PrP peptides containing this sequence have been presented (22, 23, 33). In these studies, PrP residues 113–120 have been found to adopt either parallel in-register or antiparallel β -structure, with Ala side chains of opposing strands packing into various “steric zippers” as described by Eisenberg and co-workers (34). The fact that various backbone and side chain packing polymorphs of this segment have been identified in highly similar peptides illustrates that PrP sequences are compatible with numerous amyloid conformations, a property essential to the existence and transformation of prion strains and transmissibility barriers (16, 17, 35).

The truncated PrP variant PrP23–144 is associated with a familial prion protein amyloidosis (13). Even though this specific prionopathy appears to be noninfectious (36), PrP23–144 has been a valuable *in vitro* model for investigating various aspects of protein amyloidogenesis and prion-like conformational inheritance (16), despite the fact that the β -sheet core of PrP23–144 does not overlap with that of full-length PrP amyloids generated *in vitro* (37–39). Here, we have used this protein to test the role of the 113–120 sequence in the context of a “large” prion protein with other known β -sheet forming sequences. Earlier work demonstrated that residues 113–120 become incorporated into the β -sheet core of PrP23–144 fibrils (18). Intriguingly, however, the present data reveal that deletion of these residues does not abolish (or even affect the kinetics of) fibrillogenesis or alter PrP23–144 seeding capability (Fig. 1). Thus, counterintuitively, it appears that the N-terminal part of the β -core of PrP23–144 is not critical for amyloidogenesis. In contrast, mutations or natural species-specific sequence variations near the C terminus of this protein (residues 138–139) have been shown to profoundly affect the amyloid conformation, cross-seeding capability, and fibrillization kinetics of PrP23–144 (14–16), and C-terminally truncated mutants end-

ing at residue 138 or lower were found incapable of forming amyloid (14). These findings led us to designate the region around residues 138–139 as a critical amyloidogenic determinant for PrP23–144, and recent crystallographic work on shorter PrP peptides encompassing this region (40) has provided a plausible structural explanation for how this sequence may regulate fibril nucleation in the truncated PrP fragment.

Importantly, this critical region of PrP23–144 exists in a β -strand that is mostly conserved between [WT] and [Δ 113–120] fibrils (Fig. 4C). This C-terminal β -strand, approximately residues 130–140, may therefore be considered an essential component of the PrP23–144 amyloid core, as it controls nucleation of the PrP23–144 amyloid structure (accounting for the identical fibrillization kinetics and seeding capability of [WT] and [Δ 113–120] amyloids). The β -strand region containing residues 113–120, conversely, is nonessential to amyloid nucleation (Fig. 1). In other words, not all portions of the β -sheet core contribute equally to the properties of the amyloid.

Previous studies have shown that certain conformational features of PrP23–144 variants are transmissible upon cross-seeding, whereas others are not (16, 26). Thus, the finding that both WT and Δ 113–120 PrP23–144 variants are mutually capable of seeding one another despite differences in the amyloid core sequence raises the question of whether the conformational differences resulting from deletion of residues 113–120 are transmissible to WT protein upon cross-seeding WT PrP23–144 with Δ 113–120 PrP23–144 amyloid (or vice versa). Detailed structural properties of such cross-seeded fibrils are currently under investigation by variety of techniques including multidimensional solid-state NMR spectroscopy.

Segmental Polymorphism in Nonessential Core Sequence, “Movable Core” for PrP23–144 Fibrils—In a thorough study of the islet amyloid polypeptide, Wiltzius *et al.* (41) showed that this protein exhibits so-called “segmental polymorphism”, or variability in which amino acid sequences become incorporated into the β -strand of the core (7). Mutation of islet amyloid polypeptide shifted the amyloid core to a different segment of the islet amyloid polypeptide sequence; the small size of this peptide precluded the coexistence of more than one core β -strand per islet amyloid polypeptide molecule, however. Here, we have directly demonstrated a similar segmental polymorphism within the nonessential β -strands of the PrP23–144 amyloid core, but with conservation of the essential β -strand. Residues ~106–111, which are not part of the amyloid core of [WT] fibrils, become incorporated into the core region of [Δ 113–120] fibrils, forming a nonessential part of the core of approximately the same size as that in [WT] fibrils (Fig. 4C). The essential C-terminal strand, however, is nearly conterminous (to within the ability of solid-state NMR chemical shifts to predict secondary structure) in both PrP23–144 variants. Thus, the nonessential core is movable in the sense that it can incorporate different residues under different conditions. Somewhat similar “movement” of part of the β -core was inferred (from isotope-edited FTIR spectra) to underlie pH-dependent polymorphism in fibrils of a β_2 -microglobulin peptide (42), though that study did not distinguish essential and nonessential sheets.

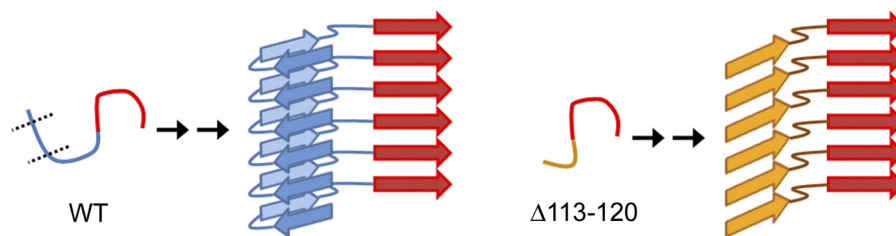


FIGURE 5. **Schematic structural model depicting movement of the amyloid β -sheet core following partial deletion of a core sequence in PrP23–144.** *Left*, amyloidogenesis of WT PrP23–144. The essential and nonessential regions of the amyloid core are shown as red and blue ribbons, respectively. *Right*, amyloidogenesis of Δ 113–120 PrP23–144. Deletion of part of the nonessential core (indicated by dotted lines in the left panel) results in a rearrangement of this part of the core (gold ribbons) with conservation of the essential core (red ribbons). The depiction of parallel in-register β -structure for [WT] and [Δ 113–120] fibrils is based on the intermolecular alignment found for [WT] fibrils (20), although no data of this type are yet available for [Δ 113–120] amyloid. The arrangement of β -strands in this figure for both fibril types is completely arbitrary and cannot be determined from the present data.

The nonessential, movable portion of the amyloid core, though it does not influence fibril formation, has a considerable influence over the conformation and ultrastructure of the amyloid fibril product (Figs. 2 and 3). This finding mirrors earlier work on PrP23–144, in which we found that the Met/Val polymorphism at position 129, located in a flexible non- β segment of the core region (18), imparts a conformational difference (visible in FTIR spectra) on PrP23–144 amyloids without affecting the fibrillization kinetics or seeding capability (26). It was concluded that sequence variation outside the nucleation-determining region can influence fibril conformation without affecting amyloidogenesis. Importantly, the present results show that this can also be true for structural or sequence differences within the rigid β -strands in the amyloid core, provided that such differences are limited to the nonessential region of the core (Fig. 5). The existence of essential and nonessential (movable) regions of a β -sheet core suggests that the concept of an amyloid core domain is not as well defined for large proteins as for small peptides. This view is supported by the finding that the β -core of fibrils formed by PrP90–231 and PrP23–231 is shifted C-terminally relative to PrP23–144 (mapping to residues \sim 160–220, Refs. 37–39), and the existence of variable-sized β -core sequences in other amyloid proteins, such as the yeast prion Sup35 (for which the core size determines strain (43–45)) or the bacterial hydrogenase maturation factor HypF (46). Our present results provide an intriguing new means by which this core variability can be achieved.

Implications for Amyloid Biochemistry—In protein misfolding diseases, amyloid toxicity may result from loss of function of the aggregated protein, association of fibrils (or small aggregates) into insoluble plaques, overloading of the protein disposal machinery, recruitment of other substances (e.g. lipid membranes or soluble proteins), or any combination of the above (1, 5, 47). In many cases, these parameters depend intimately on the physicochemical properties of amyloid aggregates (48, 49). Correspondingly, functional protein amyloids (1, 6, 8) may rely on a specific fibril conformation to achieve a particular activity or gain of function. It has been proposed (7) that structural polymorphism in both types of amyloids acts to tune the functional or toxic properties of the amyloid aggregate, either through direct changes in physicochemical properties (e.g. fibril hydrophobicity) or through variable interactions with other factors (e.g. disaggregating molecular chaperones). Several forms of amyloid polymorphism, ranging from simple side-chain rotations to large changes in the size of the β -core, have

been described (7, 34, 41, 46, 50). Our finding that segmental polymorphism can exist in a nonessential portion of an amyloid core, with conservation of an essential (nucleation-determining) portion, suggests another basis for such polymorphism. In particular, the present results demonstrate a means by which amyloid conformation and biophysical properties can vary with conservation of aggregation propensity and seeding capability. The present results are also of relevance to the emerging biotechnological applications of amyloids (51, 52), as it may be possible to achieve a desired physical property of amyloid fibrils (e.g. hydrophilicity) with retention of seeding ability, by manipulating nonessential segments of the amyloid core. It is worth noting, for example, that [Δ 113–120] fibrils lack the tendency of [WT] fibrils to form insoluble precipitate.

Because high resolution three-dimensional structural information is not yet available for PrP23–144 fibrils, it is unclear precisely how partial movement of the nonessential β -sheet core produces the marked conformational and morphological differences between [Δ 113–120] and [WT] fibrils. Undoubtedly, the structural influence of the nonessential core depends on the overall topology of the β -structure in the amyloid fibril, which can vary enormously from one protein to another (7, 10); not all amyloid structures may be compatible with the coexistence of essential and nonessential core regions. Further restrictions on the “movability” of the amyloid core may be imposed by the mechanism of structural templating of soluble protein by the amyloid seed, a process that has not been characterized in detail for any amyloid protein. Thus, although the present study shows an interesting means by which amyloid structures can display structural polymorphism, far more detailed structural and biophysical investigation is needed before the full implications of movable amyloid core sequences can be fully appreciated.

REFERENCES

- Chiti, F., and Dobson, C. M. (2006) *Annu. Rev. Biochem.* **75**, 333–366
- Pepys, M. B. (2001) *Philos. Trans. R. Soc. Lond. B Biol. Sci.* **356**, 203–210
- Westermarck, P., Andersson, A., and Westermarck, G. T. (2011) *Physiol. Rev.* **91**, 795–826
- Cobb, N. J., and Surewicz, W. K. (2009) *Biochemistry* **48**, 2574–2585
- Caughey, B., and Lansbury, P. T. (2003) *Annu. Rev. Neurosci.* **26**, 267–298
- Gebbink, M. F., Claessen, D., Bouma, B., Dijkhuizen, L., and Wösten, H. A. (2005) *Nat. Rev. Microbiol.* **3**, 333–341
- Greenwald, J., and Riek, R. (2010) *Structure* **18**, 1244–1260
- Shewmaker, F., McGlinchey, R. P., and Wickner, R. B. (2011) *J. Biol. Chem.* **286**, 16533–16540
- Auer, S., Dobson, C. M., and Vendruscolo, M. (2007) *HFSP J.* **1**, 137–146

Polymorphism in Y145Stop Prion Protein Amyloids

- Miller, Y., Ma, B., and Nussinov, R. (2010) *Chem. Rev.* **110**, 4820–4838
- Wiltzius, J. J., Landau, M., Nelson, R., Sawaya, M. R., Apostol, M. I., Goldschmidt, L., Soriaga, A. B., Cascio, D., Rajashankar, K., and Eisenberg, D. (2009) *Nat. Struct. Mol. Biol.* **16**, 973–978
- Bucciantini, M., Giannoni, E., Chiti, F., Baroni, F., Formigli, L., Zurdo, J., Taddei, N., Ramponi, G., Dobson, C. M., and Stefani, M. (2002) *Nature* **416**, 507–511
- Kitamoto, T., Iizuka, R., and Tateishi, J. (1993) *Biochem. Biophys. Res. Commun.* **192**, 525–531
- Kundu, B., Maiti, N. R., Jones, E. M., Surewicz, K. A., Vanik, D. L., and Surewicz, W. K. (2003) *Proc. Natl. Acad. Sci. U.S.A.* **100**, 12069–12074
- Vanik, D. L., Surewicz, K. A., and Surewicz, W. K. (2004) *Mol. Cell* **14**, 139–145
- Jones, E. M., and Surewicz, W. K. (2005) *Cell* **121**, 63–72
- Surewicz, W. K., Jones, E. M., and Apetri, A. C. (2006) *Acc. Chem. Res.* **39**, 654–662
- Helmus, J. J., Surewicz, K., Nadaud, P. S., Surewicz, W. K., and Jaroniec, C. P. (2008) *Proc. Natl. Acad. Sci. U.S.A.* **105**, 6284–6289
- Helmus, J. J., Surewicz, K., Surewicz, W. K., and Jaroniec, C. P. (2010) *J. Am. Chem. Soc.* **132**, 2393–2403
- Helmus, J. J., Surewicz, K., Apostol, M. I., Surewicz, W. K., and Jaroniec, C. P. (2011) *J. Am. Chem. Soc.* **133**, 13934–13937
- Gasset, M., Baldwin, M. A., Lloyd, D. H., Gabriel, J. M., Holtzman, D. M., Cohen, F., Fletterick, R., and Prusiner, S. B. (1992) *Proc. Natl. Acad. Sci. U.S.A.* **89**, 10940–10944
- Lee, S. W., Mou, Y., Lin, S. Y., Chou, F. C., Tseng, W. H., Chen, C. H., Lu, C. Y., Yu, S. S., and Chan, J. C. (2008) *J. Mol. Biol.* **378**, 1142–1154
- Walsh, P., Simonetti, K., and Sharpe, S. (2009) *Structure* **17**, 417–426
- Norstrom, E. M., and Mastrianni, J. A. (2005) *J. Biol. Chem.* **280**, 27236–27243
- Morillas, M., Swietnicki, W., Gambetti, P., and Surewicz, W. K. (1999) *J. Biol. Chem.* **274**, 36859–36865
- Jones, E. M., Surewicz, K., and Surewicz, W. K. (2006) *J. Biol. Chem.* **281**, 8190–8196
- Nadaud, P. S., Helmus, J. J., and Jaroniec, C. P. (2007) *Biomol. NMR Assign.* **1**, 117–120
- Delaglio, F., Grzesiek, S., Vuister, G. W., Zhu, G., Pfeifer, J., and Bax, A. (1995) *J. Biomol. NMR* **6**, 277–293
- Goddard, T. D., and Kneller, D. G. (2006) SPARKY 3, University of California, San Francisco, CA
- Byler, D. M., and Susi, H. (1986) *Biopolymers* **25**, 469–487
- Shen, Y., Delaglio, F., Cornilescu, G., and Bax, A. (2009) *J. Biomol. NMR* **44**, 213–223
- Moore, R. A., Herzog, C., Errett, J., Kocisko, D. A., Arnold, K. M., Hayes, S. F., and Priola, S. A. (2006) *Protein Sci.* **15**, 609–619
- Kuwata, K., Matumoto, T., Cheng, H., Nagayama, K., James, T. L., and Roder, H. (2003) *Proc. Natl. Acad. Sci. U.S.A.* **100**, 14790–14795
- Sawaya, M. R., Sambashivan, S., Nelson, R., Ivanova, M. I., Sievers, S. A., Apostol, M. I., Thompson, M. J., Balbirnie, M., Wiltzius, J. J., McFarlane, H. T., Madsen, A. Ø., Riek, C., and Eisenberg, D. (2007) *Nature* **447**, 453–457
- Tanaka, M., Chien, P., Yonekura, K., and Weissman, J. S. (2005) *Cell* **121**, 49–62
- Tateishi, J., and Kitamoto, T. (1995) *Brain Pathol.* **5**, 53–59
- Cobb, N. J., Sönnichsen, F. D., McHaourab, H., and Surewicz, W. K. (2007) *Proc. Natl. Acad. Sci. U.S.A.* **104**, 18946–18951
- Lu, X., Wintrod, P. L., and Surewicz, W. K. (2007) *Proc. Natl. Acad. Sci. U.S.A.* **104**, 1510–1515
- Tycko, R., Savtchenko, R., Ostapchenko, V. G., Makarava, N., and Baskakov, I. V. (2010) *Biochemistry* **49**, 9488–9497
- Apostol, M. I., Wiltzius, J. J., Sawaya, M. R., Cascio, D., and Eisenberg, D. (2011) *Biochemistry* **50**, 2456–2463
- Wiltzius, J. J., Sievers, S. A., Sawaya, M. R., Cascio, D., Popov, D., Riek, C., and Eisenberg, D. (2008) *Protein Sci.* **17**, 1467–1474
- Hiramatsu, H., Lu, M., Goto, Y., and Kitagawa, T. (2010) *Bull. Chem. Soc. Japan* **83**, 495–504
- Toyama, B. H., Kelly, M. J., Gross, J. D., and Weissman, J. S. (2007) *Nature* **449**, 233–237
- Verges, K. J., Smith, M. H., Toyama, B. H., and Weissman, J. S. (2011) *Nat. Struct. Mol. Biol.* **18**, 493–499
- Tessier, P. M., and Lindquist, S. (2009) *Nat. Struct. Mol. Biol.* **16**, 598–605
- Wang, L., Schubert, D., Sawaya, M. R., Eisenberg, D., and Riek, R. (2010) *Angew. Chem. Int. Ed. Engl.* **49**, 3904–3908
- Voisine, C., Pedersen, J. S., and Morimoto, R. I. (2010) *Neurobiol. Dis.* **40**, 12–20
- Mossuto, M. F., Dhulesia, A., Devlin, G., Frare, E., Kumita, J. R., de Laureto, P. P., Dumoulin, M., Fontana, A., Dobson, C. M., and Salvatella, X. (2010) *J. Mol. Biol.* **402**, 783–796
- Yoshiike, Y., Akagi, T., and Takashima, A. (2007) *Biochemistry* **46**, 9805–9812
- Paravastu, A. K., Leapman, R. D., Yau, W. M., and Tycko, R. (2008) *Proc. Natl. Acad. Sci. U.S.A.* **105**, 18349–18354
- Channon, K., and MacPhee, C. E. (2008) *Soft Matter* **4**, 647–652
- Cherny, I., and Gazit, E. (2008) *Angew. Chem. Int. Ed. Engl.* **47**, 4062–4069